

Energy consumption of an electro dialyzer desalinating aqueous polymer solutions

P.A. Sosa-Fernandez^{a,b,c}, T.M. Loc^a, M. Andrés-Torres^a, M. Tedesco^a, J.W. Post^a, H. Bruning^{b,*}, H.H.M. Rijnaarts^b

^a Wetsus, European centre of excellence for sustainable water technology, P.O. Box 1113, 8911 CC Leeuwarden, the Netherlands

^b Wageningen University, Sub-Department of Environmental Technology, P.O. Box 8129, 6700 EV Wageningen, the Netherlands

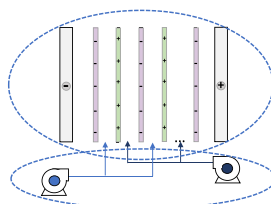
^c Wageningen University, Physical Chemistry and Soft Matter, P.O. Box 8038, 6700 EK Wageningen, the Netherlands

HIGHLIGHTS

- Electrodialysis of highly viscous fluids was experimentally investigated.
- Effects of spacer thickness, fluid viscosity, salinity, and linear velocity considered
- Increase in overall energy consumption only for high viscosity feeds + thin spacers

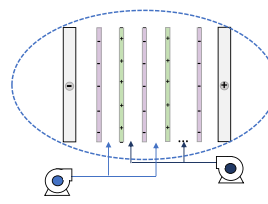
GRAPHICAL ABSTRACT

Thin spacers (300 μm) + low salinity (1 g/L) and high viscosity feed (12 cP)



DESALINATION ENERGY \sim PUMPING ENERGY

Spacers thicker than 300 μm , feed salinity > 1 g/L, feed viscosity < 12 cP



DESALINATION ENERGY \gg PUMPING ENERGY

ARTICLE INFO

Keywords:

Electrodialysis
Electrodialyzer
Energy-consumption
Pumping energy
Viscosity

ABSTRACT

When performing electrodialysis (ED) to desalinate a stream, both the energy for desalination and the energy for pumping contribute to the total energy consumption, although under typical working conditions (e.g., brackish water desalination) the latter is usually negligible. However, the energy penalty might increase when desalinating viscous mixtures (i.e., viscosity of 2–20 cP). In this work, we experimentally investigate the desalination performance of an ED-unit operating with highly viscous water-polymer mixtures. The contribution of desalination and pumping energy to the total energy consumption was measured while varying diverse parameters, i.e., salinity and viscosity of the feed, and geometry and thickness of the spacer. It was found that the type of spacer did not significantly influence the energy required for desalination. The pumping energy was higher than predicted, though in most cases minimal compared to the energy for desalination. Only when using thin spacers (300 μm) and/or highly viscous feeds (12 cP), the pumping energy accounted for 50% of the total energy for low salinity feeds. Therefore, the main contributor to the energy consumption of viscous solutions is the desalination energy, provided that large spacer thicknesses (at least 450 μm) and adequate operating conditions are utilized to limit pumping energy losses.

* Corresponding author.

E-mail address: harry.bruning@wur.nl (H. Bruning).

1. Introduction

Electrodialysis (ED) is a mature process applied in industrial scale for the production of potable water from brackish water sources for more than 50 years [1,2]. Since then, electrodialysis has been used in an increasing variety of applications, such as production of table salt [3], recovery of organic acids [4], and for the desalination of industrial streams. Most of these industrial applications address the desalination of aqueous streams with low viscosity, so the operation of the electro-dialyzer does not differ much from desalting brackish water. However, new applications for ED are rapidly emerging, such as removal of lactic acid from acid whey [5], desalination of glycerol [6], of fish sauce [7], and of viscous produced water from the oil and gas industry [8]. These applications have in common the high viscosity of the feed solutions, typically in the range of 2–20 cP, i.e., several times higher than sea or brackish water. In electrodialysis, the viscosity of the feed solution may influence not only the mass transfer between the solution and the membranes and hence the energy required for desalination [9,10], but also the energy required to pump the feed through the electro-dialyzer. In our previous works we have used synthetic viscous water from the oil industry and presented preliminary economic calculations for the cost of desalination [11,12]. However, in the case of high-viscosity solutions the relative contributions for desalination and for pumping in the total energy consumption have not been specifically addressed. Therefore, there is an evident need to study the electrodialysis of viscous feeds, focusing on the influence of several parameters in the energy consumption.

Electrodialysis uses an applied electrical potential difference as driving force to desalinate one of the streams circulating through an electro-dialyzer, which consists of a series of anion and cation exchange membranes (AEMs and CEMs, respectively) placed alternately between two electrodes and separated by spacers. During operation, the electrodes are polarized and an electrical field is generated between them, which allows the cations to migrate towards the cathode passing through the CEMs. Likewise, the anions migrate towards the anode passing through the AEMs while the desalting and concentrating solution flow between these membranes. Thus, the electrical potential difference at the electrodes allows ion transport in the electro-dialyzer, resulting in a net transport of ions from the dilute compartment to the concentrate compartment [1,13].

The energy consumed by electrodialysis can be attributed to two main contributions, i.e. pumping and desalination [14]. The energy required to transport ions from the dilute to concentrate (desalination energy) depends on the system performance, which is mainly determined by the electrical resistance of the membranes and the solutions. In most cases, the highest resistance in the system is due to the diffusive boundary layers close to the surface of the membranes in the dilute compartment. Due to the non-homogeneous mixing of the solutions at the proximities of IEMs, concentration polarization occurs, thus causing diffusion boundary layers of non-negligible thickness inside the channel. Concentration polarization phenomena in ED are enhanced when the current density increases. In particular, a limiting condition is reached when the ion concentration at the membrane/solution interface approaches zero, and the corresponding current value is known as limiting current density [15–17].

Spacers play an important role for both energy contributions. They are placed between the ion-exchange membranes to create a constant intermembrane distance and to improve the mixing of the solutions inside the compartments. The use of spacers can also have some disadvantages, like covering part of the membrane and reducing the area available for ion conduction, a phenomenon called shadow effect [18]. On the one hand, thinner spacers are preferred to reduce the electric resistance in the compartments [19], but on the other hand thinner spacers also lead to increased pressure drop and higher risk of irreversible fouling. Thus, the selection of spacer thickness is crucial to enhance the process performance under given process and feed

conditions. Another option is the use of spacer-less cell design, by using profiled membranes [20,21], which allow to reduce pressure drops [22] and potentially minimizing the risk of fouling, though less effective than conventional spacers to promote mixing in the channels [23].

When using viscous solutions in ED, their friction forces are higher than for non-viscous solutions. Hence, larger pressure losses than for other aqueous systems should be expected. However, assessing the pressure loss in an electro-dialyzer is not an easy task. This has been recently pointed out by Wright et al. [24], who created a comprehensive model for brackish water desalination, but who admitted not being able to find a model that reliably predicted pressure drop in the flow channels. For this reason, the authors concluded that it is necessary to keep pressure drop and pumping energy characterization for ED stacks as an ongoing area of research.

Therefore, it is of special interest to investigate what are the main constraints when employing ED to desalinate highly viscous solutions. For instance, in the case of viscous produced water from the oil and gas industry, the feed solution could initially have a water-like viscosity (i.e. in the range of 1–2 mPa-s) while increasing significantly (up to 20 cP) after the ED step [8]. Such a large increase of viscosity between inlet and outlet can remarkably impact the overall energy consumption of ED, as well as the optimal operating conditions of the process.

The aim of this work is to assess the energy consumption of electro-dialysis with highly viscous streams (up to 12 mPa-s), by investigating the effect of different parameters, both on the feed conditions (flow rate, viscosity, salinity), and on the cell geometry (spacer thickness). We experimentally tested an ED unit equipped with spacers of different thicknesses (ranging between 300 and 720 μm) and fed with NaCl and polymer solutions at different salt concentration (1 and 5 g/L NaCl) and viscosities (1, 2, 5 and 12 mPa-s), at different flowrates. Finally, we evaluate the desalination performance of the system, by identifying suitable working conditions to limit pumping losses when desalinating viscous solutions via electro-dialysis.

2. Materials and methods

2.1. Materials

2.1.1. Electro-dialysis stack

Desalination experiments were performed in a $10 \times 10 \text{ cm}^2$ electro-dialysis stack with cross-flow configuration for the feed streams (REDstack B.V., The Netherlands). The stack contained 10 membrane pairs, each one composed by one CEM, one AEM, and two spacers. The membranes in the stack were Fujifilm CEM and AEM Type 10 (Fujifilm Manufacturing Europe B.V., The Netherlands), while Neosepta CMX membranes (Astom Corp., Japan) were used as outer CEMs (close to the electrodes). Once placed in the stack, each membrane had a working area of 100 cm^2 . The outer membranes were separated from the electrode compartments by 300 μm gaskets. The electrodes, placed at the end plates, were made of titanium with Ru/Ir oxide coating (Magneto Special Anodes B.V., The Netherlands). The stack was closed by the two end plates and tightened to a 6 Nm torque. The final sealing of the stack was ensured by using silicon glue. A schematic drawing of the stack and experimental setup can be found in [25].

The ion exchange membranes used in this work (Fujifilm AEM/CEM type 10) are homogenous ion exchange membranes based on polyolefin with strong functional groups (quaternary ammonium for the AEM and sulfonic acid for the CEM). The membranes have low electric resistance and high permselectivity [26], with characteristics summarized in Table 1. Before the experiments, the membranes were conditioned in 0.1 M NaCl solution for 5 days.

2.1.2. Spacers

Four different spacers were used in this work, one extruded and three woven, as shown in Fig. 1. Their main properties are summarized in Table 2. All the thickness values reported in Table 2 were measured with

Table 1

Properties of the anion and cation exchange membranes employed in this study. Data taken from their suppliers.

Membrane property	AEM type 10	CEM type 10
Backbone chemistry	Acrylamide	Acrylamide
Thickness dry (μm)	125	135
Area resistance ($\Omega \text{ cm}^2$, measured in 0.5 M NaCl)	1.7	2.0
Permselectivity (measured at 0.05–0.5 M NaCl)	95	99
pH stability	1–13	1–13

a digital caliper (Mitutoyo 547-401, Japan). The extruded spacers (Deukum GmbH, Germany) were 300 μm thick, while the three kinds of woven spacers (AquaBattery B.V., The Netherlands) had thicknesses of 300, 450, and 720 μm , respectively. The void fraction (ϵ) reported in Table 2 was calculated using the following equation [24]:

$$\epsilon = 1 - \frac{\pi d_f^2}{2l_f h} \quad (1)$$

where d_f is the diameter of the fiber, l_f is the distance between two fibers and h is the spacer thickness, all obtained from the netting data.

2.1.3. Solutions

Table 3 summarizes the main properties of the solutions used during this study. They comprised two different salinities and four values of viscosity (μ). Two different salinity values were chosen, to mimic the typical composition of polymer-flooding produced water [8,28]. The salinities employed were 5.0 g/L NaCl, namely ‘brackish water’ (BW), and 1.0 g/L NaCl, referred as ‘low salinity water’ (LSW). The mentioned viscosities, measured at 25 °C, were attained by adding 1.0 to 4.0 g/L of non-ionic polyacrylamide (NPAM). The density of all solutions was ~ 1.0 g/L. It is worth noting that NPAM, being a non-ionic compound, does not affect the electrical conductivity of the solution (see Table 3). Each experiment required 25 L of concentrate and 25 L of diluate solution. The polymer-containing solutions were prepared by first hydrating the NPAM in a flask containing 10 L of salt solution, and then diluting it to reach 25 L of feed solution with the desired viscosity. The experiment was executed within 2 days of preparing the feed solutions

to avoid degradation of the polymer.

The sodium chloride was analytical grade, provided by VWR (The Netherlands). The non-ionic polymer NPAM was Flopaam FA920 (MW of 5–7 million Da), kindly provided by SNF (France). This non-ionic polymer was chosen over the hydrolyzed one used in previous studies [8,11], to limit the electrostatic interactions with the charged membranes. The electrode rinse solution (ERS) consists of an aqueous solution of sodium sulfate 20 g/L, which was continuously recirculated between anode and cathode for all the tests.

2.2. Methods

2.2.1. Electrodialysis tests

The electrodialysis experiments were conducted in continuous mode (single pass) at a constant voltage of 3.0 V supplied and controlled by a potentiostat (IVIUMnSTAT, Ivium Technologies, The Netherlands). Four different stacks, each one assembled with a different type of spacer, were employed to desalinate the feed solutions as summarized in Table 3. During each ED experiment, the diluate and concentrate solutions were circulated at the same flowrate, varied between 50 and 300 mL/min, by two independent pumps (Masterflex L/S). The electrode rinse solution was pumped by a third pump at a constant rate of 170 mL/min. All the experiments were run at room temperature (23 ± 1 °C). During each experiment, voltage, current, and conductivities of the diluate and concentrate streams were continuously recorded. The pressure difference between inlet and outlet of the diluate stream was measured by means of two pressure sensors (Jumo, Germany) positioned immediately before and after the stack.

After each experiment, the stack was cleaned-in-place by circulating a sequence of solutions, each one during 10 min at a flow rate of 200 mL/min. The procedure comprised: HCl solution (pH = 2), 0.1 M NaCl, NaOH solution (pH = 12), 0.1 M NaCl, and finally a 5.0 g/L NaCl solution. This cleaning procedure was chosen to guarantee the removal of polymer from the membranes, since it has been suggested that NaOH is more effective in removing polyacrylamide fouling from CEMs while HCl is better in removing this kind of fouling from the AEM [29].

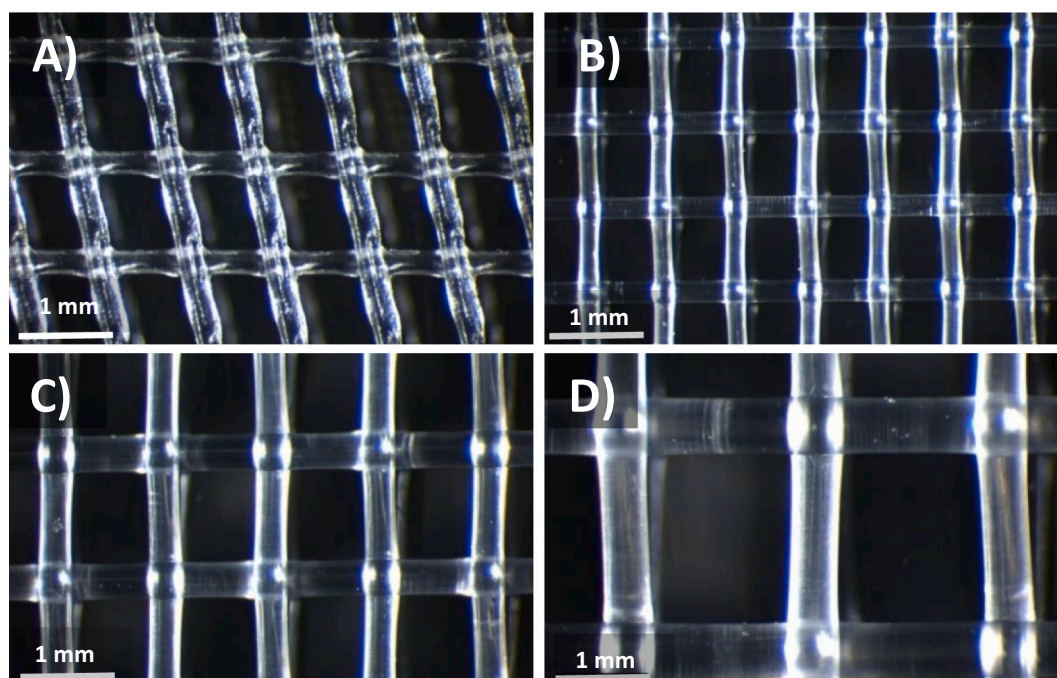


Fig. 1. The four spacers used during this study: A) 300 μm , extruded; B) 300 μm woven; C) 450 μm woven; D) 720 μm woven.

2.2.2. Composition and viscosity analyses

Samples from the feed and the diluate outlet were regularly taken during each test. The chloride concentration was measured by ion chromatography (IC, Compact IC, Metrohm), while sodium was measured by inductive-coupled plasma method (ICP-OES, Optima 5300DV, Perkin Elmer).

Viscosity curves of the feed and diluate solutions were measured at different shear rates with a rheometer (RheoCompass, Anton Paar) using the bob and cup configuration. All samples were stored at 5 °C and measured at 25 °C within 5 days.

2.2.3. Calculation of desalination performance and pressure drops

For each flow rate, samples from the outlet of the diluate solution were taken by triplicate (approximately after 15, 20, and 25 min for each test) to independently measure their Na⁺ and Cl⁻ content, as previously described. Next, the average removal for each sample was calculated based on the ion removal of Na⁺ and Cl⁻, as expressed in Eq. (2):

$$\text{ion removal} = \frac{1}{2} \left[\left(1 - \frac{n_{dil}^{Na}}{n_{feed}^{Na}} \right) + \left(1 - \frac{n_{dil}^{Cl}}{n_{feed}^{Cl}} \right) \right] \times 100\% \quad (2)$$

where n_{dil}^{Na} and n_{dil}^{Cl} are, respectively, the number of moles of Na⁺ and Cl⁻ in the diluate of the sample; and $\overline{n_{feed}^{Na}}$ and $\overline{n_{feed}^{Cl}}$ are the average number of moles of Na⁺ and Cl⁻ in the feed solution, determined as average from 3 samples. Since the feed contains a binary electrolyte (NaCl), the ion removal for Na and Cl should be the same. In fact, the concentration of Cl and Na as measured via IC and ICP-OES were very similar for all the samples, besides minor deviations (<1%) that are in line with experimental scattering and sampling accuracy. Finally, the ion removal at each flow rate was averaged also from 3 independent samples.

The linear velocity of the fluid in the channel u (m/s) was calculated using Eq. (3) [24]:

$$u = \frac{Q}{\varepsilon w h N} \quad (3)$$

where Q is the total volumetric flow rate (m³/s), ε is the spacer void fraction (-), w is the cell width ($w = 0.1$ m, in this study), h is the spacer thickness (m) and N is the number of cell pairs ($N = 10$).

The Reynolds number (Re) was calculated for a flow between two parallel flat plates, as described by Wright et al. [24]:

$$Re = \frac{2\rho u h}{\mu} \quad (4)$$

where ρ is the density of the solution (kg/m³). The viscosity values used for the calculations were those reported in Table 3.

The desalination energy E_{des} (Wh/m³) required for each flowrate Q_d (m³/h) was calculated as follows:

$$E_{des} = \frac{U \int_0^t I \cdot dt}{Q_d \cdot t} \quad (5)$$

where U is the applied voltage (V) measured across the cell pairs (excluding the electrodes), I is the current (A) and t is the base time (1 h). Both I and U were experimentally recorded by the Ivium-n-Stat.

The pressure drops ΔP (Pa) between two parallel plates can be modelled by means of the Darcy-Weisbach equation, which relies on the

Table 2

Main characteristics of the spacers used in this work.

Identifier	Nominal thickness (μm)	Open area (%)	Material	Void fraction ε	Supplier
300 extruded	300	–	Polypropylene	0.77	Deukum GmbH
300 woven	300	56	Polyamide	0.70	AquaBattery B.V.
450 woven	450	53	Polyamide	0.71	AquaBattery B.V.
720 woven	720	59	Polyamide	0.76	AquaBattery B.V.

Table 3

Description and properties of the investigated feed solutions.

Viscosity μ (cP)	Case I Brackish water (BW) 5.0 g/L NaCl		Case II Low salinity water (LSW) 1.0 g/L NaCl	
	NPAM concentration, cNPAM (g/L)	Conductivity, σ (mS/cm)	NPAM concentration, cNPAM (g/L)	Conductivity, σ (mS/cm)
1.0	0	9.36	0	2.21
2.0	1.0	9.47	1.0	2.20
5.0	2.0	9.49	2.0	2.23
12.0	3.8	9.25	3.8	2.26

fluid density ρ , the Darcy friction factor f (-), the length of the channel's active area L (m), the fluid velocity in the channel u , and the spacer thickness h (m) [24]:

$$\Delta P = \frac{\rho f L u^2}{4h} \quad (6)$$

The friction factor f was calculated using the model developed by Gurreri et al. [30], and later adopted by Wright et al. [24]. Based on the results presented by Wright et al., this represents the most accurate model so far reported in predicting the pressure drop of a bench-scale ED stack.

The energy consumed for pumping a fluid was determined from the flow rates and the pressure drop ΔP in each stream, expressed as:

$$E_{pump} = \frac{Q_d \cdot \Delta P_d + Q_c \cdot \Delta P_c}{Q_d \cdot k_{eff}} \quad (7)$$

In which E_{pump} (Wh/m³) is the pumping energy consumption for the diluate and concentrate streams [14], k_{eff} (-) is the efficiency of the pumps, while Q_d and Q_c are the total flow rates (m³/h) of diluate and concentrate, and ΔP_d and ΔP_c the corresponding pressure drops (Pa). In Eq. (7), the pressure drop in the electrode rinse is neglected due to the small volume of electrode rinse solution compared with the volumes of the diluate and concentrate solutions.

3. Results and discussion

3.1. Energy consumption for desalination

The electro dialysis experiments were run at constant voltage, so the first indication of differences in performance was the attained current density. An example of the initial data obtained is included in Figs. S1 and S2, which present, respectively, the current densities recorded when desalting 5.0 and 1.0 g/L NaCl solutions with different viscosities and in the different stacks tested. The current density increased with time since the flowrate was being increased. This was expected since a shorter residence time will lead to a lower desalination degree in the stack (under single-pass configuration). In addition, high flow rates improve hydrodynamics in the compartments, thus reducing concentration polarization phenomena [17]. The effect of both phenomena is lower resistance and hence higher current density with higher flow rate. Furthermore, for the experiments desalinating the solutions with 5.0 g/L NaCl, the current densities attained were higher than for the 1.0 g/L NaCl solutions, as expected given the higher conductivity.

Next, using the samples collected during the experiments and Eq. (1),

the average ion removal was calculated for each stack, solution, and flow condition. The average fluid velocity in the stack was calculated using Eq. (2) and the spacer specifications. The results hereby obtained are presented in Fig. 2 as ion removal versus linear velocity u for the different spacers and solutions.

It is worth noticing that the ion removals included in Fig. 2 are consistent with the current densities shown in Figs. S1 and S2, which suggests also constant current efficiency during the runs. All plots in Fig. 2 also show decreased ion removal as the fluid velocity increases due to the decreasing residence time. Fig. 2 also shows that different spacers allowed very different ion removal: while the 450 μm spacer yielded up to 90% ion removal, the 300 μm woven spacer did not allow to remove more than 20% of the ions present in the feed. When comparing the 300 μm spacers, it can be observed that the ion removal using extruded spacers was approximately 3 times higher than when

using the woven one. This could be due to the fluid channelling and not wetting the entire membrane area available. It should be also noted 300 μm -woven and 300 μm -extruded spacers have different mesh orientation (45 and 90, respectively), which influences the mass transfer in the compartments [30,31]. The highest ion removal values were achieved with the stack containing 450 μm woven spacers, which can be attributed to a better flow distribution in the stack, and consequently a higher current efficiency. It also results noteworthy that the percentages of ion removal only varied depending on the spacer and were very similar for solutions with the same viscosity and different salinity.

Fig. 2 also shows that, for most cases, higher ion removals were obtained when desalting solutions with higher viscosity. The higher ion removals also correspond with the higher current densities reported in Figs. S1 and S2. This might be due to different flow regimes: on one hand one would expect higher concentration polarization with higher

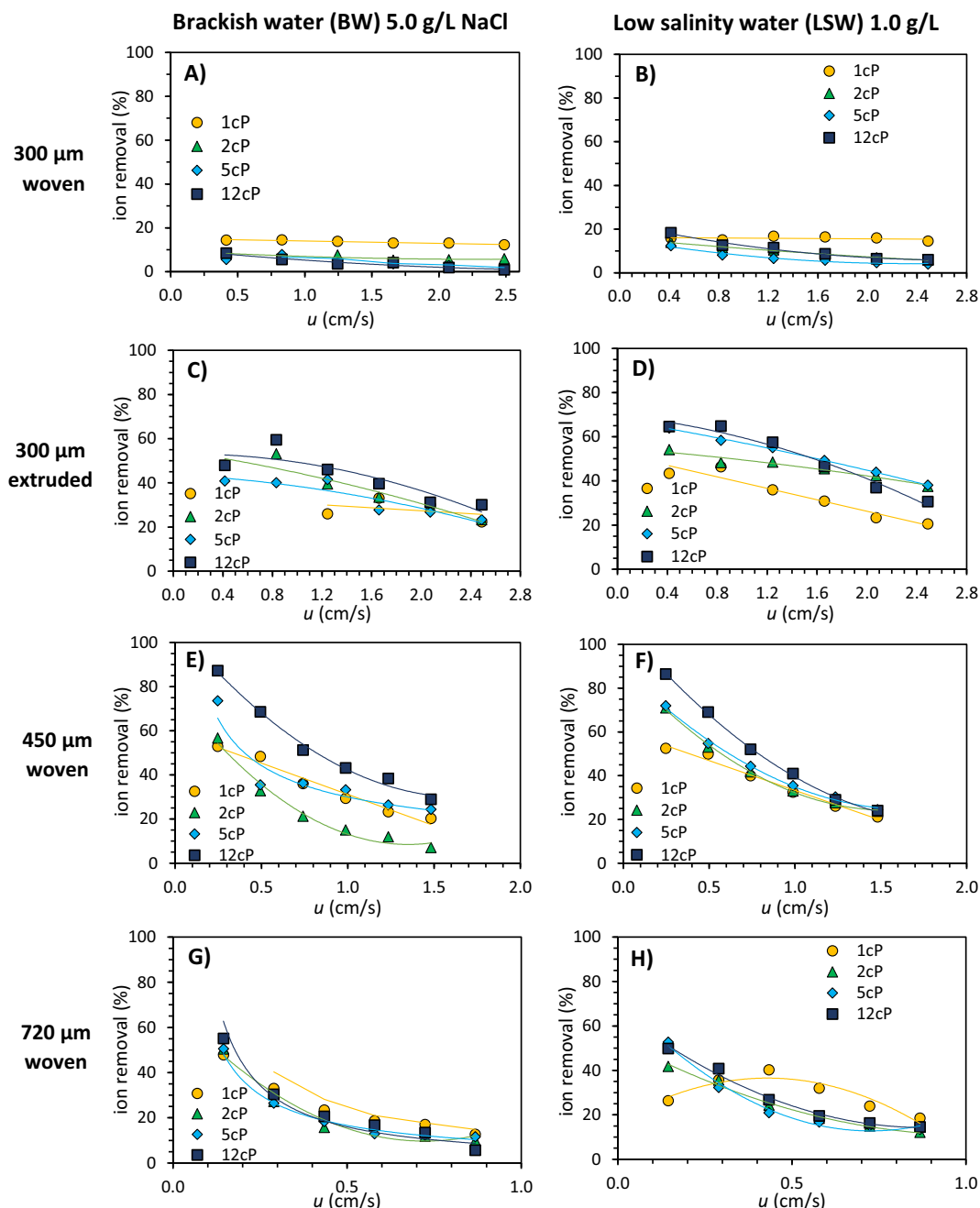


Fig. 2. Ion removal (%) versus linear velocity for desalination experiments of NaCl solutions with different viscosities performed at constant voltage (3.0 V).

viscosity (i.e. a lower current density), but on the other hand the higher viscosity may lead to a better flow distribution over the stack (i.e. a higher current density). Due to fouling or irregularities on the membrane surface, the flow through some areas of the electro dialyzer may become restricted, a phenomenon known as preferential channelling [32]. Thus, given the lower performance observed for the stacks with the 300 μm woven spacers, one might conclude that preferential channelling occurred during those experiments.

As shown in Fig. 2, the ion removal values and current densities varied as a function of the solution viscosity and type of spacers. Consequently, the desalination energy consumption E_{des} , calculated using Eq. (3), also varied. This can be observed in Fig. 3, where the

energy is plotted against the average ion removal.

Fig. 3 shows that the energy for desalination E_{des} is linearly dependent of the amount of the percentage of removed ions, independently of the viscosity of the solution or the spacer in the stack. In other words, in the investigated (under-limiting) current regime, the current efficiency remains constant in all the tests. This is expected to occur for experiments at constant voltage, because any increase in resistance does not lead to above average heat losses, but only to a lower current (density). Therefore, since the energy consumption E_{des} is directly related to the current (Eq. (5)) and the latter is linked to the number of ions transported (Eqs. (8) and (9)), the relationship between E_{des} and ion removal is linear, as expressed in Eq. (10). Table S1 in the Supplementary

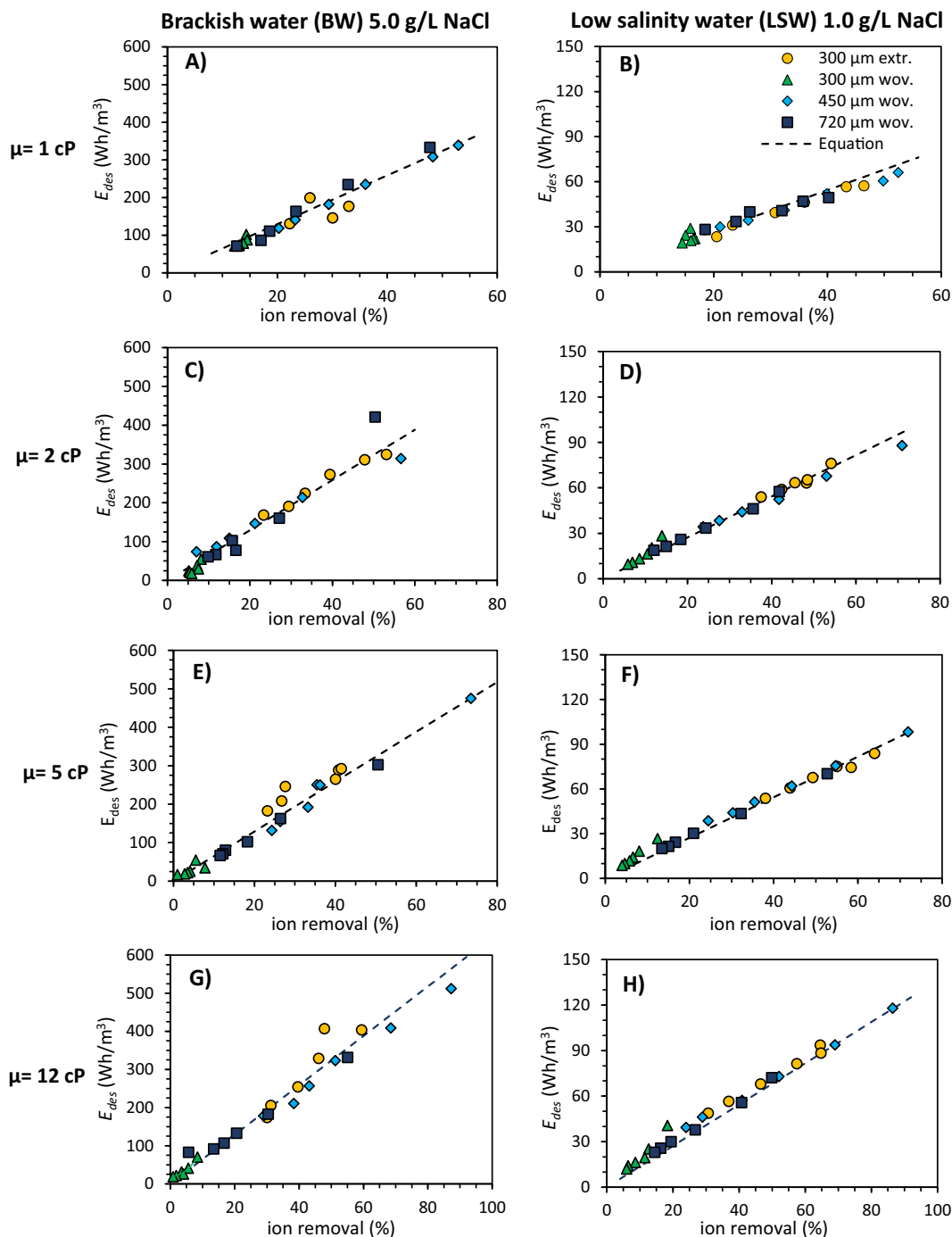


Fig. 3. Specific energy consumption vs. ion removal for electro dialysis experiments desalinating solutions containing 5.0 and 1.0 g/L NaCl with additional NPAM at different concentration.

material compares the analytical solution for Eq. (10) and the empirical solution (obtained from the trendlines in Fig. 3).

$$I = Q \times F \times (C_{in} - C_{out}) \tag{8}$$

$$E_{des} = U \times F \times (C_{in} - C_{out}) \tag{9}$$

$$E_{des} = U \times F \times C_{in} \times \text{ion removal} \tag{10}$$

3.2. Pressure loss and energy for pumping

Fig. 4 includes the experimentally measured pressure drops for the diluate side of the four stacks. Higher pressure drops occurred on the stacks with thinner spacers (smaller h) and for higher flow velocities, as expected when considering Eq. (6). The pressure drop was also higher when the viscosity of the diluate was higher, which causes a higher friction factor f .

Besides the experimental data, Fig. 4 also includes the pressure drop calculated by the model developed by Gurreri et al. [30], and later adapted by Wright et al. [24] (as described in Section 2.2.3). It can be observed that the model underestimate ΔP , most notoriously for the 720 μm spacer and for the higher viscosities. Indeed, Wright et al. also reported an underestimation of the pressure drop when using Gurreri's et al. and other models, although in their case the differences were less significant [24]. In this case, the friction factor calculated by the model would need to be approximately three times higher to predict more accurately the experimental data here presented.

Our first hypothesis to explain such discrepancy between model and data was that, since the model was developed specifically for low-viscosity solutions with Newtonian behaviour, its predictions of pressure loss when a fluid with higher viscosity might be compromised. Indeed, polymer solutions are usually non-Newtonian fluids, with apparent viscosity increasing as the shear rate increases, making more difficult to predict the pressure loss due to friction. However, by plotting

the calculated friction factor versus the Reynolds number (Fig. 5), it was observed that the same f/Re relationship holds for all data independently of the viscosity, meaning that the polymer-salt solutions used in this work all have Newtonian behaviour in the investigated range of shear rates. Therefore, it can be concluded that the difference between model and experiments are not due to different rheological behaviour of the investigated solutions. Instead, such discrepancy is most likely due to the concentrated pressure drops (in the inlet-outlet manifolds of the stack), which are measured experimentally but not included in the model [30,33]. In that regard, our results are similar to the ones of Gurreri et al., who also reported higher pressure drops for the manifolds that for the inner part of the cell [33].

The energy needed to pump the diluate and concentrate solutions through the electro dialyzer was calculated using Eq. (7) (ΔP_d , Q_d , ΔP_c , Q_c and $k_{eff} = 0.9$). The results obtained for the low salinity case are presented in Fig. 6 as a function of the linear velocity u . The results are closely related to those presented in the previous figure: larger pumping energies are required when treating fluids with higher viscosity, as well as when using thinner spacers. It is worth noticing that the pumping energies for the 450 and the 720 μm spacers are very similar, while the one obtained for 300 μm woven spacer is significantly different from the other two spacers, especially for viscosities of 2 cP or higher. It might be that the results with the 300 μm woven spacers were different due to the orientation of the spacer. The force applied to close the stack could have pushed the spacer netting into the membrane, especially at the inlet and outlet of the membrane pile. Then, due to the 90 degree orientation of the spacer, the remaining flow channel between the wires of the woven netting and the membrane is much narrower, heavily obstructing the feed flow.

3.3. Total energy consumption

Fig. 7 presents the total energy consumption needed to remove 50% of the ions from the low salinity solutions (1.0 g/L NaCl), calculated by

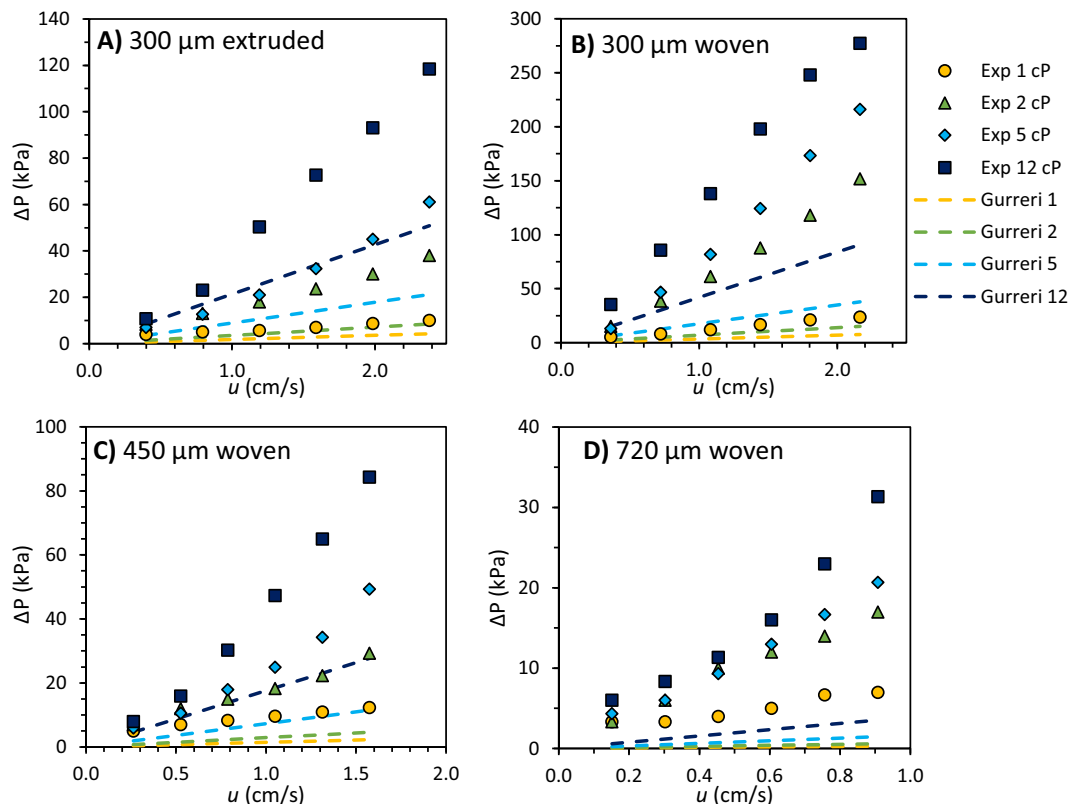


Fig. 4. Model and experimental pressure drop for the 4 stacks tested with solutions of 1, 2, 5, and 12 cP.

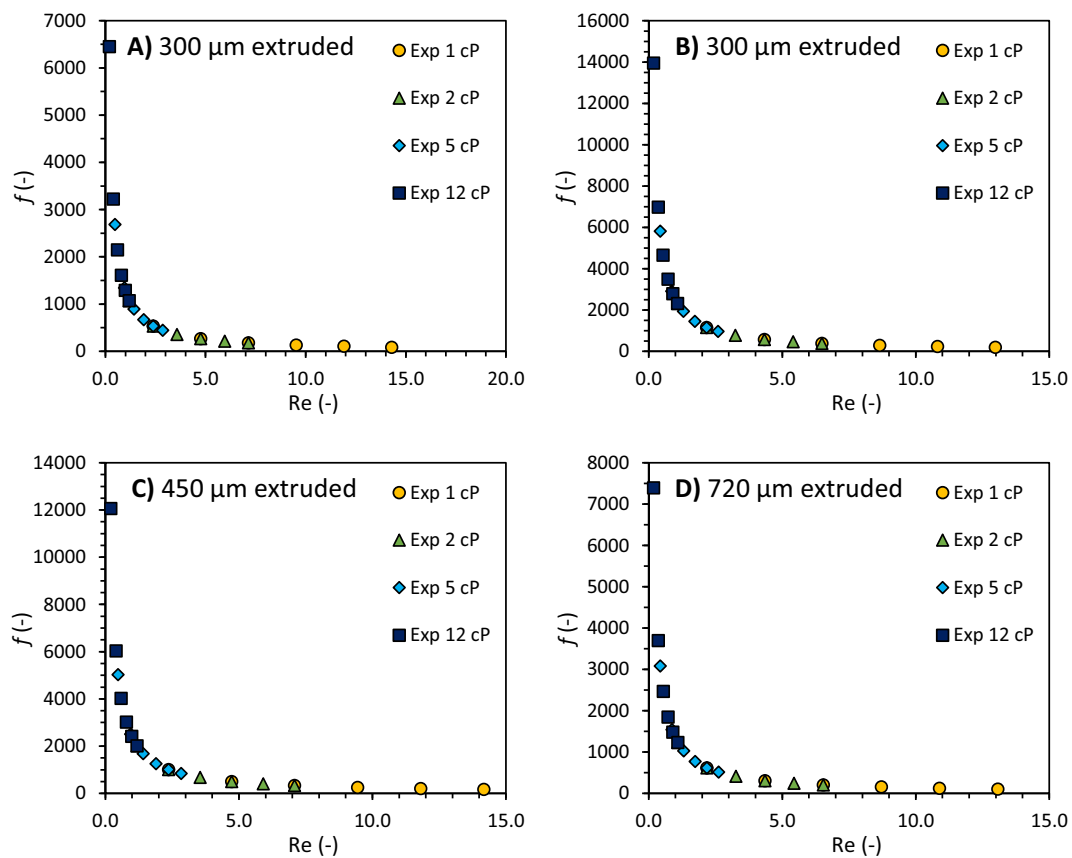


Fig. 5. Friction factor versus Re for the 4 stacks tested with solutions of 1, 2, 5, and 12 cP.

adding the desalination and pumping energy consumptions. It shows that, for all the studied cases, E_{des} is larger than E_{pump} , and in particular when using 450 or 720 μm spacers to desalinate solutions with viscosities up to 5 cP, the pumping energy can be practically considered negligible. However, when employing any of the 300 μm spacers, or when desalting the streams with higher viscosity (12 cP) the E_{pump} value becomes more relevant, even matching the E_{des} value in the case of the 12 cP solution with the 300 μm extruded spacer.

When analysing the results obtained for the BW solution it should be considered that the desalination energy is approximately 5 times larger than for the LSW, while the energy for pumping is the same. Therefore, for the BW solution the main contribution to energy consumption was in all cases the desalination energy. These results are included in the Supplementary material.

3.4. Evaluation of fluid viscosity after ED

Besides the main energy requirements of the process, there is another constraint when pumping viscous solutions: the sensitivity of the feed solutions to shear. In the case of polymer-containing solutions, high shear rates can cause breaking of the polymer and reduction of the viscosity [34]. To evaluate this effect, the viscosity of the feed and the diluate solutions was determined after all the ED experiments.

The viscosity measurements are presented in Fig. 8 as a function of shear rate. It shows that all the diluate outlet solutions had the same viscosity as the initial feed solution, independently of the spacer thickness or fluid velocity at which they were treated. This result confirms that the shear forces inside the stack do not cause any significant breaking of the polymer chains. There could be the possibility that due to the decrease in the salt content, the viscosity of the diluate increases and was compensated for the possible polymer degradation. However, even in the case of low ion removal (e.g., the 300 μm woven stack), the

outlet solutions presented the same viscosity as the feed. These results are similar to those of Kalbani et al., who studied the degradation of polyacrylamide solutions and found minimal viscosity decreases when passing the solutions through a centrifugal pump. In that case, they found to be more efficient to cause a drastic pressure drop by means of a valve, or to use chemical oxidation [34].

4. Conclusions

In this work, we assess the energy consumption for the desalination and pumping of viscous fluids using ED stacks with different type of spacers. Specifically, we tested polymer-water mixture with varying viscosity (1–12 cP) and salinity (1 and 5 g/L), which resulted in different current densities and ion removal. However, when compared for the same output of 50% ion removal, results indicated practically equal energy consumption for all viscosities and spacer configurations tested, indicating no additional energy needs for desalination.

The results showed an evident effect of spacer configuration and fluid viscosity on the pumping energy consumption. The pumping energy became a significant component (in some cases up to 48%) in the total energy need when solutions of viscosity above 1 cP (1 mPa·s) were desalinated, especially when desalting 12 cP solutions. Nevertheless, the only case in which the measured pumping energy consumption was equal to the desalting energy consumption was when desalting a 1 g/L NaCl solution of 12 cP in a stack containing 300 μm -thick spacers.

The results obtained indicated that, in most cases, desalinating viscous streams (in the range of 2–12 cP) via ED gives negligible pumping energy requirements, given that flow rate and spacer geometry are properly chosen. Specifically, spacers of 450 μm are preferable to obtain lower pumping energy (E_{pump}) consumption while achieving high salt removal. Furthermore, spacers with moderate thicknesses would also be beneficial for processes where there is fouling formation, since in

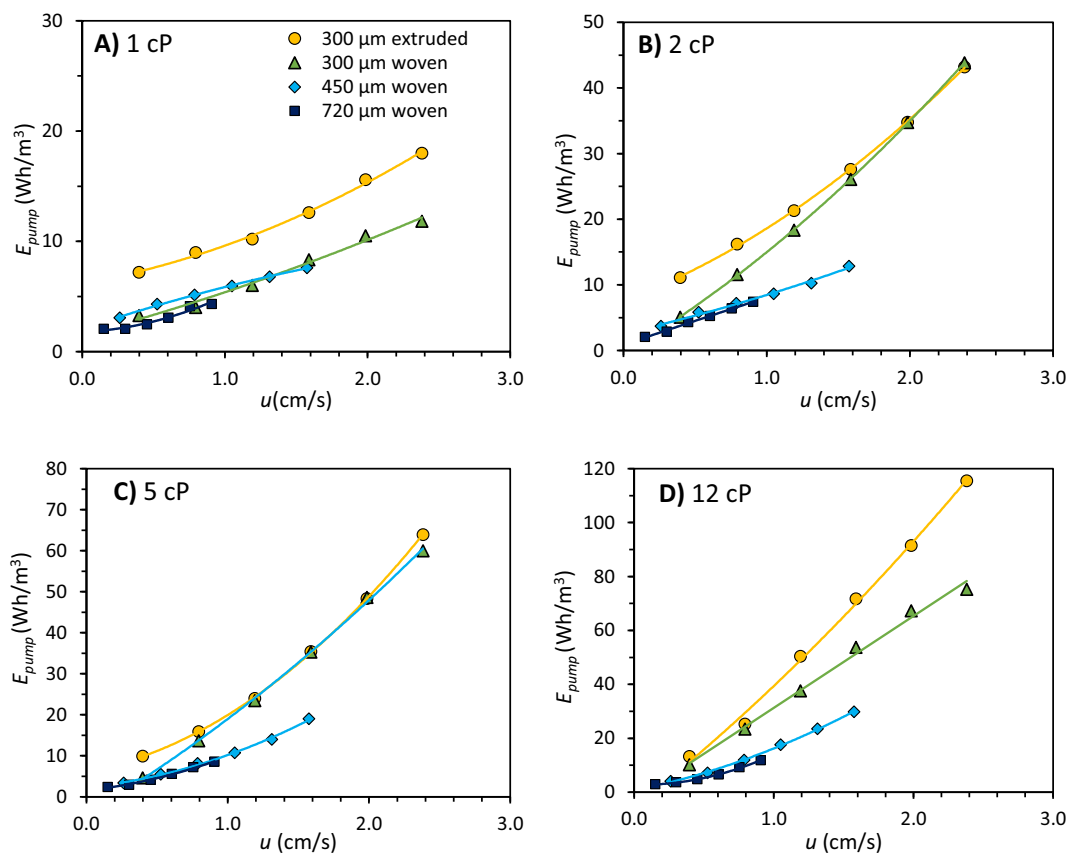


Fig. 6. Pumping energy consumption as a function of linear velocity u for the case of LSW solution (1 g/L NaCl).

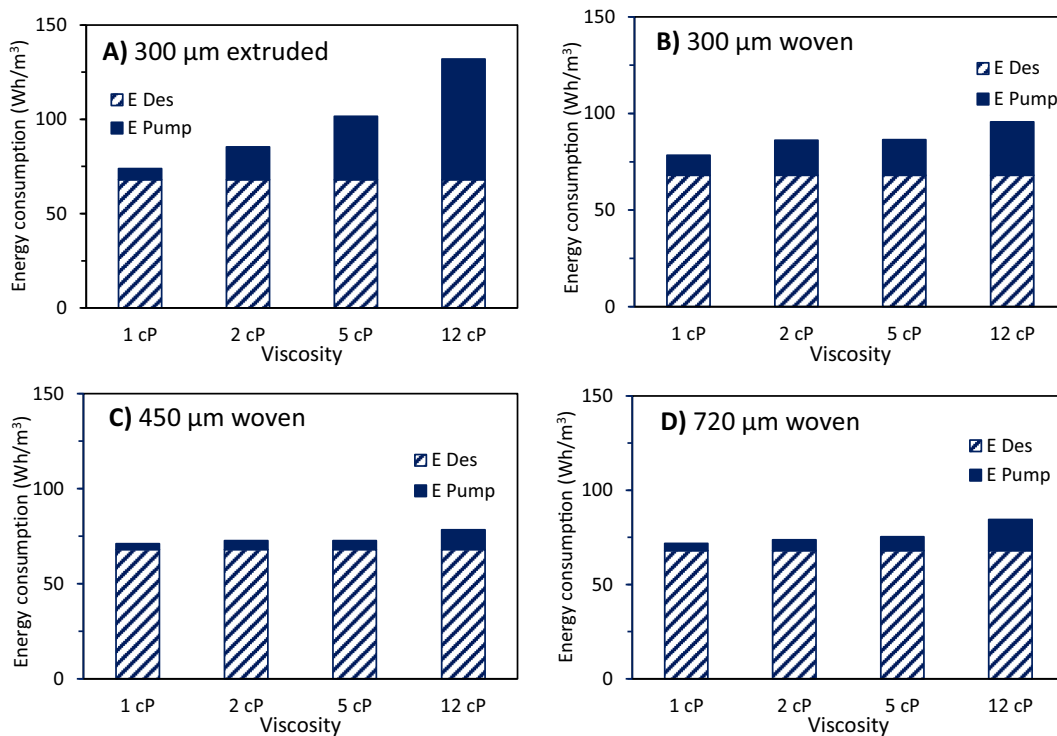


Fig. 7. Total energy consumption to remove 50% of the salt from 1.0 g/L NaCl solutions, calculated for feed solutions at different viscosity and type of spacer.

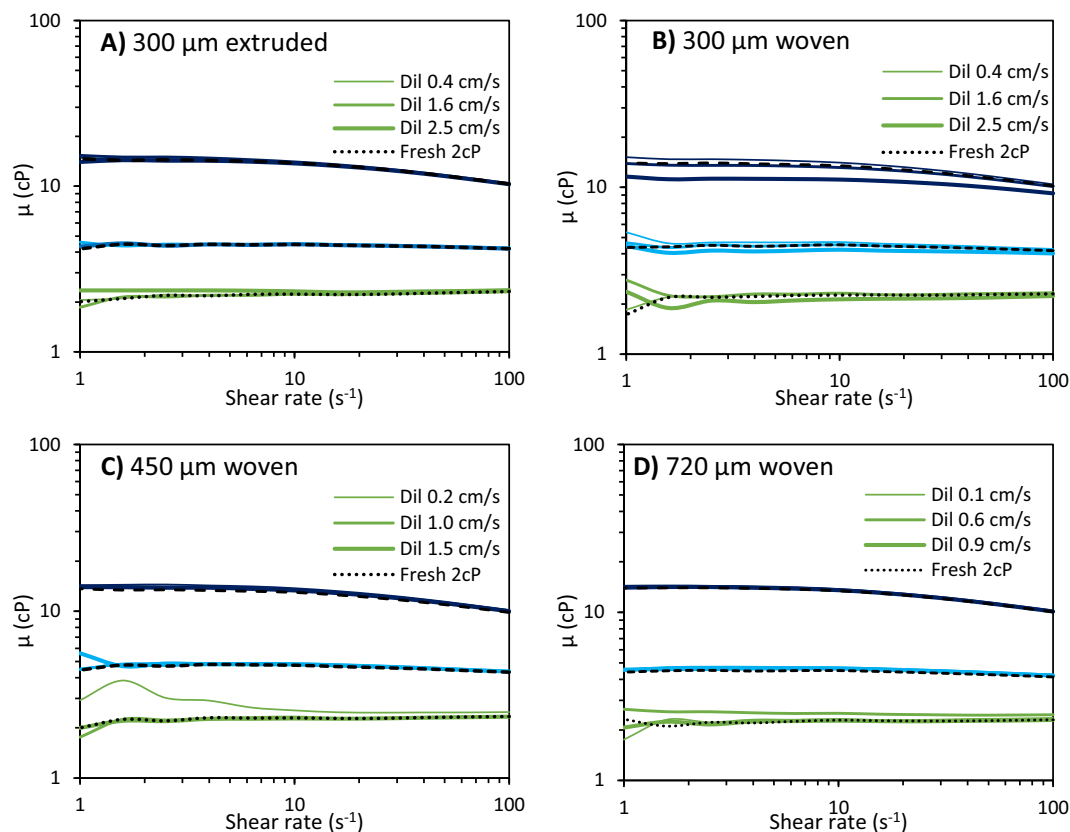


Fig. 8. Viscosity of the feed and diluate solutions as function of shear rate. The plots show the measurements for LSW solutions (1 g/L NaCl+NPAM) viscosified at 2, 5 and 12 cP. The viscosity was measured for each of the flowrates tested, but only 50, 200 and 300 mL/min (expressed as fluid velocity) are shown. A) 300 μm extruded spacer, B) 300 μm woven, C) 450 μm woven and D) 720 μm woven.

those cases the pressure drop might be more severe.

In addition, this study proved that no polymer breakage occurred during the desalinations performed, and for any of the experimental conditions. Finally, we propose that future research should include a larger range of fluid velocities during the runs, as well as to explore alternative options to handle highly viscous fluids, like working at higher temperatures.

CRediT authorship contribution statement

P.A. Sosa-Fernandez: Conceptualization; Data curation; Formal analysis; Investigation; Methodology; Supervision; Validation; Visualization; Roles/Writing - original draft.

T.M. Loc: Formal analysis; Investigation; Methodology.

M. Andrés-Torres: Formal analysis; Investigation; Methodology.

M. Tedesco: Conceptualization; Formal analysis; Methodology; Supervision; Writing - review & editing.

J.W. Post: Conceptualization; Formal analysis; Funding acquisition; Methodology; Supervision; Project administration; Resources; Writing - review & editing.

Bruning: Conceptualization; Formal analysis; Project administration; Supervision; Writing - review & editing.

H.H.M. Rijnaarts: Conceptualization; Formal analysis; Funding acquisition; Supervision; Writing - review & editing.

Declaration of competing interest

The authors declare that they have no known competing financial interests or personal relationships that could have appeared to influence the work reported in this paper.

Acknowledgments

This work was performed in the cooperation framework of Wetsus, European Centre of Excellence for Sustainable Water Technology (www.wetsus.nl). Wetsus is co-funded by the Dutch Ministry of Economic Affairs and Ministry of Infrastructure and Environment, the European Union Regional Development Fund, the Province of Fryslân, and the Northern Netherlands Provinces. This research has received funding from the European Union's Horizon 2020 - Research and Innovation Framework Programme under the H2020 Marie Skłodowska-Curie Actions grant agreement No 665874. We are grateful to the participants of the research theme "Desalination" for fruitful discussions and financial support. The authors would like to thank S. Grasman and K. Goeting for their useful comments to improve the manuscript.

Appendix A. Supplementary data

Supplementary data to this article can be found online at <https://doi.org/10.1016/j.desal.2021.115091>.

References

- [1] H. Strathmann, Electrodialysis, a mature technology with a multitude of new applications, *Desalination*. 264 (2010) 268–288, <https://doi.org/10.1016/j.desal.2010.04.069>.
- [2] A. Campione, L. Gurreri, M. Ciofalo, G. Micale, A. Tamburini, A. Cipollina, Electrodialysis for water desalination: a critical assessment of recent developments on process fundamentals, models and applications, *Desalination*. 434 (2018) 121–160, <https://doi.org/10.1016/j.desal.2017.12.044>.
- [3] T. Kawahara, K. Suzuki, Utilization of the waste concentrated seawater in the desalination plants, *Desalination*. 38 (1981) 499–507.
- [4] C. Huang, T. Xu, Y. Zhang, Y. Xue, G. Chen, Application of electrodialysis to the production of organic acids: state-of-the-art and recent developments, *J. Membr. Sci.* 288 (2007) 1–12, <https://doi.org/10.1016/j.memsci.2006.11.026>.

- [5] G.Q. Chen, F.I.I. Eschbach, M. Weeks, S.L. Gras, S.E. Kentish, Removal of lactic acid from acid whey using electrodialysis, *Sep. Purif. Technol.* 158 (2016) 230–237, <https://doi.org/10.1016/j.seppur.2015.12.016>.
- [6] P. Vadthya, A. Kumari, C. Sumana, S. Sridhar, Electrodialysis aided desalination of crude glycerol in the production of biodiesel from oil feed stock, *Desalination*. 362 (2015) 133–140, <https://doi.org/10.1016/j.desal.2015.02.001>.
- [7] J. Chen, M. Li, R. Yi, K. Bai, G. Wang, R. Tan, S. Sun, N. Xu, Electrodialysis extraction of pufferfish skin (*Takifugu flavidus*): a promising source of collagen, *Mar. Drugs* 17 (2019) 1–15, <https://doi.org/10.3390/md17010025>.
- [8] P.A. Sosa-Fernandez, J.W. Post, H. Bruning, F.A.M. Leermakers, H.H.M. Rijnaarts, Electrodialysis-based desalination and reuse of sea and brackish polymer-flooding produced water, *Desalination*. 447 (2018) 120–132, <https://doi.org/10.1016/j.desal.2018.09.012>.
- [9] O. Kuroda, S. Takahashi, M. Nomura, Characteristics of flow and mass transfer rate in an electrodialyzer compartment including spacer, *Desalination*. 46 (1983) 225–232.
- [10] T. Huang, I. Yu, Correlation of ionic transfer rate in electrodialysis under limiting current density conditions, *J. Membr. Sci.* 35 (1988) 193–206, [https://doi.org/10.1016/S0376-7388\(00\)82443-6](https://doi.org/10.1016/S0376-7388(00)82443-6).
- [11] P.A. Sosa-Fernandez, J.W. Post, M.S. Ramdani, F.A.M. Leermakers, H. Bruning, H.H.M. Rijnaarts, Improving the performance of polymer-flooding produced water electrodialysis through the application of pulsed electric field, *Desalination*. 484 (2020), <https://doi.org/10.1016/j.desal.2020.114424>.
- [12] P.A. Sosa-Fernandez, J.W. Post, A. Karemire, H. Bruning, H.H.M. Rijnaarts, Desalination of Polymer-flooding Produced Water at Increased Water Recovery and Minimized Energy, 2020, <https://doi.org/10.1021/acs.iecr.0c02088>.
- [13] R. Valerdi-Pérez, M. López-Rodríguez, J.A. Ibáñez-Mengual, Characterizing an electrodialysis reversal pilot plant, *Desalination*. 137 (2001) 199–206, [https://doi.org/10.1016/S0011-9164\(01\)00219-3](https://doi.org/10.1016/S0011-9164(01)00219-3).
- [14] H. Strathmann, Assessment of electrodialysis water desalination process costs, Proceedings of the International Conference on Desalination Costing, Lemassol, Cyprus, December 6–8, 2004. (2004) 32–54.
- [15] V.V. Nikonenko, A.V. Kovalenko, M.K. Urtenov, N.D. Pismenskaya, J. Han, P. Sistat, G. Pourcelly, Desalination at overlimiting currents: state-of-the-art and perspectives, *Desalination*. 342 (2014) 85–106, <https://doi.org/10.1016/j.desal.2014.01.008>.
- [16] A.M. Peers, General discussion, Discussions of the Faraday Society. 1956 (1956) 124–125.
- [17] M. La Cerva, L. Gurreri, M. Tedesco, A. Cipollina, M. Ciofalo, A. Tamburini, G. Micale, Determination of limiting current density and current efficiency in electrodialysis units, *Desalination*. 445 (2018) 138–148, <https://doi.org/10.1016/j.desal.2018.07.028>.
- [18] H. Strathmann, *Ion-exchange Membrane Separation Processes, First*, Elsevier, B.V., Amsterdam, 2004.
- [19] D.A. Vermaas, M. Saakes, K. Nijmeijer, Doubled power density from salinity gradients at reduced intermembrane distance, *Environ. Sci. Technol.* 45 (2011) 7089–7095, <https://doi.org/10.1021/es2012758>.
- [20] S. Pawlowski, J.G. Crespo, S. Velizarov, Profiled ion exchange membranes: a comprehensive review, *Int. J. Mol. Sci.* 20 (2019), <https://doi.org/10.3390/ijms20010165>.
- [21] C. Larchet, V.I. Zabolotsky, N. Pismenskaya, V.V. Nikonenko, A. Tskhay, K. Tastanov, G. Pourcelly, Comparison of different ED stack conceptions when applied for drinking water production from brackish waters, *Desalination*. 222 (2008) 489–496, <https://doi.org/10.1016/j.desal.2007.02.067>.
- [22] D.A. Vermaas, M. Saakes, K. Nijmeijer, Power generation using profiled membranes in reverse electrodialysis, *J. Membr. Sci.* 385–386 (2011) 234–242, <https://doi.org/10.1016/j.memsci.2011.09.043>.
- [23] L. Gurreri, M. Ciofalo, A. Cipollina, A. Tamburini, W. Van Baak, G. Micale, CFD modelling of profiled-membrane channels for reverse electrodialysis, *Desalin. Water Treat.* 55 (2015) 3404–3423, <https://doi.org/10.1080/19443994.2014.940651>.
- [24] N.C. Wright, S.R. Shah, S.E. Amrose, A.G. Winter, A robust model of brackish water electrodialysis desalination with experimental comparison at different size scales, *Desalination*. 443 (2018) 27–43, <https://doi.org/10.1016/j.desal.2018.04.018>.
- [25] J. Moreno, N. de Hart, M. Saakes, K. Nijmeijer, CO₂ saturated water as two-phase flow for fouling control in reverse electrodialysis, *Water Res.* 125 (2017) 23–31, <https://doi.org/10.1016/j.watres.2017.08.015>.
- [26] P.A. Sosa-Fernandez, S.J. Miedema, H. Bruning, F.A.M. Leermakers, H.H.M. Rijnaarts, J.W. Post, Influence of solution composition on fouling of anion exchange membranes desalinating polymer-flooding produced water, *J. Colloid Interface Sci.* 557 (2019) 381–394, <https://doi.org/10.1016/j.jcis.2019.09.029>.
- [27] L. Henthorne, G.A. Pope, U. Weerasooriya, V. Llano, Impact of water softening on chemical enhanced oil recovery, in: Proceedings - SPE Symposium on Improved Oil Recovery 2014, SPE, Tulsa, Oklahoma, 2014.
- [28] C. Wang, W. Ming, D. Yan, C. Zhang, M. Yang, Y. Liu, Y. Zhang, B. Guo, Y. Wan, J. Xing, Novel membrane-based biotechnological alternative process for succinic acid production and chemical synthesis of bio-based poly (butylene succinate), *Bioresour. Technol.* 156 (2014) 6–13, <https://doi.org/10.1016/j.biortech.2013.12.043>.
- [29] L. Gurreri, A. Tamburini, A. Cipollina, G. Micale, M. Ciofalo, Flow and mass transfer in spacer-filled channels for reverse electrodialysis: a CFD parametrical study, *J. Membr. Sci.* 497 (2016) 300–317, <https://doi.org/10.1016/j.memsci.2015.09.006>.
- [30] F.N. Ponzio, A. Tamburini, A. Cipollina, G. Micale, M. Ciofalo, Experimental and computational investigation of heat transfer in channels filled by woven spacers, *Int. J. Heat Mass Transf.* 104 (2017) 163–177, <https://doi.org/10.1016/j.ijheatmasstransfer.2016.08.023>.
- [31] D.A. Vermaas, M. Saakes, K. Nijmeijer, Early detection of preferential channeling in reverse electrodialysis, *Electrochim. Acta* 117 (2014) 9–17, <https://doi.org/10.1016/j.electacta.2013.11.094>.
- [32] L. Gurreri, A. Tamburini, A. Cipollina, G. Micale, M. Ciofalo, Pressure drop at low Reynolds numbers in woven-spacer-filled channels for membrane processes: CFD prediction and experimental validation, *Desalin. Water Treat.* 61 (2017) 170–182, <https://doi.org/10.5004/dwt.2016.11279>.
- [33] H. Al Kalbani, M.S. Mandhari, H. Al-Hadhrami, G. Philip, J. Nesbit, L. Gil, N. Gaillard, Treating back produced polymer to enable use of conventional water treatment technologies, Society of Petroleum Engineers - SPE EOR Conference at Oil and Gas West Asia 2014: Driving Integrated and Innovative EOR. (2014) 617–629. doi:<https://doi.org/10.2118/169719-ms>.